

See discussions, stats, and author profiles for this publication at: <https://www.researchgate.net/publication/40678317>

Insight into the Mechanism of Antimicrobial Conjugated Polyelectrolytes: Lipid Headgroup Charge and Membrane Fluidity Effects

ARTICLE *in* LANGMUIR · DECEMBER 2009

Impact Factor: 4.46 · DOI: 10.1021/la9038045 · Source: PubMed

CITATIONS

42

READS

30

5 AUTHORS, INCLUDING:



Liping Ding

Shaanxi Normal University

50 PUBLICATIONS 954 CITATIONS

SEE PROFILE



Eva Chi

University of New Mexico

48 PUBLICATIONS 1,774 CITATIONS

SEE PROFILE



Kirk S Schanze

University of Florida

325 PUBLICATIONS 11,321 CITATIONS

SEE PROFILE

Insight into the Mechanism of Antimicrobial Conjugated Polyelectrolytes: Lipid Headgroup Charge and Membrane Fluidity Effects

Liping Ding,^{†,‡} Eva Y. Chi,^{*,†} Kirk S. Schanze,[§] Gabriel P. Lopez,^{*,†} and David G. Whitten^{*,†}

[†]Center for Biomedical Engineering, Department of Chemical and Nuclear Engineering, University of New Mexico, Albuquerque, New Mexico 87131-1341, [‡]Key Laboratory of Applied Surface and Colloid Chemistry of Ministry of Education, School of Chemistry and Material Science, Shaanxi Normal University, Xi'an 710062, P. R. China, and [§]Department of Chemistry, University of Florida, Gainesville, Florida 32611-7200

Received October 8, 2009. Revised Manuscript Received November 14, 2009

The interactions of antimicrobial cationic conjugated polyelectrolytes (CPEs) with two model membranes, liposomes and lipid monolayers at the air–water interface, have been investigated by fluorescence emission, fluorescence quenching, pressure–area isotherm, and dynamic light scattering measurements. This study continues the evaluation of the antimicrobial mechanism of a cationic poly(phenylene ethynylene) (PPE)-based CPE (polymer **1**), which contains a 2,5-thienylene moiety in the repeat unit. To this end, the interactions of polymer **1** with lipids with varying headgroup charge and acyl chain length have been examined. Our results show that the cationic polymer **1** can efficiently associate with and insert into anionic phosphatidylglycerol (PG) membranes. However, polymer **1** does not exhibit any interactions with zwitterionic lipid membranes composed of phosphatidylcholine (PC) and phosphatidylethanolamine (PE) lipids. Polymer **1**'s selective affinity toward anionic lipids over zwitterionic lipids makes it an attractive antimicrobial agent with low toxicity. The interactions of polymer **1** with lipid membranes of different fluidity were studied by varying the surface pressure of lipid monolayers and by adjusting the temperature of liposomes. We observe that increasing membrane fluidity enhances both the conformational changes of polymer **1** upon associating with lipid membranes and the extent of polymer **1** insertion into lipid monolayers. We also find that the thickness of the lipid bilayers, modulated by acyl chain length, affects the extent of polymer **1** incorporation into the lipid bilayer.

Introduction

There is a growing interest in designing and developing novel and effective antimicrobials to combat the increasing threats from pathogenic bacteria.^{1,2} Cationic polymers containing pendant quaternary ammonium groups have been among the most promising candidates as effective antimicrobials and biocides.³ We have recently demonstrated that poly(phenylene ethynylene) (PPE)-based cationic conjugated polyelectrolytes (CPEs) exhibit promising biocidal activity against a variety of bacteria and spores and thus have potential as new antibiotics.^{4–7} In order to better understand the antimicrobial actions of these PPE CPEs, we have examined their mechanisms of killing bacteria.^{5,7} The ability of PPE CPEs to interfacially generate singlet oxygen has been used to explain the observed oxygen dependence of their light-activated biocidal activity.^{5,6} However, certain PPE-CPEs also exhibit the remarkable ability for killing bacteria in the dark.⁷

As has been demonstrated in several studies, the biocidal activity of many antimicrobial peptides or polymers stems from their ability to associate with or insert into the bacterial cell wall, which results in

the disruption of the underlying cell membrane.^{8–10} Therefore, extensive efforts have been focused on studying the interaction of antimicrobial materials with model membranes to evaluate the mechanisms of antimicrobial action.^{11–13} We have recently examined the interaction of a thiophene CPE (polymer **1** in Scheme 1) with anionic phosphatidylglycerol (PG)-containing model membranes.¹⁴ The observed strong affinity of polymer **1** toward PG lipids and its facile insertion into PG membranes provide an explanation for its dark biocidal activity.¹⁴ It has been widely demonstrated that the interaction between antimicrobial molecules and lipid membranes is influenced by many factors, including lipid composition,¹⁵ lipid headgroup charge,¹⁶ and lipid packing.¹⁷ Therefore, we examined the effects of these factors on the interactions between PPE CPEs and lipid membranes so as to further understand the mechanism of antimicrobial action of PPE CPEs.

In the present study, we have extended our investigation of the interactions of polymer **1** with model membranes comprising

*To whom correspondence should be addressed. E-mail: whitten@unm.edu (D.G.W.); gplopez@unm.edu (G.P.L.); evachi@unm.edu (E.C.).

(1) Svenson, J.; Stensen, W.; Brandsdal, B.-O.; Haug, B. E.; Monrad, J.; Svendsen, J. S. *Biochemistry* **2008**, *47*, 3777–3788.

(2) Haug, B. E.; Stensen, W.; Kalaj, M.; Rekdal, Q.; Svendsen, J. S. *J. Med. Chem.* **2008**, *51*, 4306–4314.

(3) Kenawy, E.-R.; Worley, S. D.; Broughton, R. *Biomacromolecules* **2007**, *8*, 1359–1384.

(4) Lu, L.; Rininsland, F. H.; Wittenburg, S. K.; Achyuthan, K. E.; McBranch, D. W.; Whitten, D. G. *Langmuir* **2005**, *21*, 10154–10159.

(5) Chemburu, S.; Corbitt, T. S.; Ista, L. K.; Ji, E.; Fulghum, J.; Lopez, G. P.; Ogawa, K.; Schanze, K. S.; Whitten, D. G. *Langmuir* **2008**, *24*, 11053–11062.

(6) Corbitt, T. S.; Sommer, J. R.; Chemburu, S.; Ogawa, K.; Ista, L. K.; Lopez, G. P.; Whitten, D. G.; Schanze, K. S. *Appl. Surf. Interfaces* **2009**, *1*, 48–52.

(7) Corbitt, T. S.; Ding, L.; Ji, E.; Ista, L. K.; Ogawa, K.; Lopez, G. P.; Schanze, K. S.; Whitten, D. G. *Photochem. Photobiol. Sci.* **2009**, *8*, 998–1005.

(8) Arnt, L.; Rennie, J. R.; Linser, S.; Willumeit, R.; Tew, G. N. *J. Phys. Chem. B* **2006**, *110*, 3527–3532.

(9) Waschinski, C. J.; Barnert, S.; Theobald, A.; Schubert, R.; Kleinschmidt, F.; Hoffmann, A.; Saalwächter, K.; Tiller, J. C. *Biomacromolecules* **2008**, *9*, 1764–1771.

(10) Hadjicharalambous, C.; Sheynis, T.; Jelinek, R.; Shanahan, M. T.; Ouellette, A. J.; Gizeli, E. *Biochemistry* **2008**, *47*, 12626–12634.

(11) Epanand, R. M.; Vogel, H. J. *Biochim. Biophys. Acta* **1999**, *1462*, 11–28.

(12) Shai, Y. *Biochim. Biophys. Acta* **1999**, *1462*, 55–70.

(13) Castillo, J. A.; Pinazo, A.; Carilla, J.; Infante, M. R.; Alsina, M. A.; Haro, I.; Clapés, P. *Langmuir* **2004**, *20*, 3379–3387.

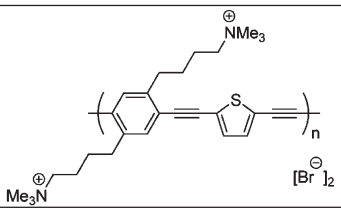
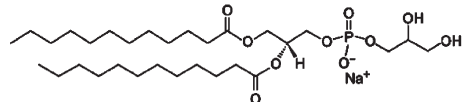
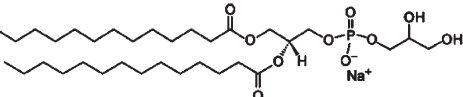
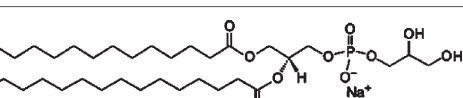
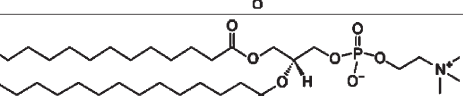
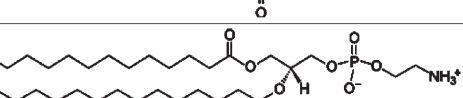
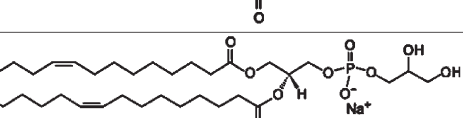
(14) Ding, L.; Chi, E. Y.; Chemburu, S.; Ji, E.; Schanze, K. S.; Lopez, G. P.; Whitten, D. G. *Langmuir*, published online June 17, <http://dx.doi.org/10.1021/la901457t>.

(15) Som, A.; Tew, G. N. *J. Phys. Chem. B* **2008**, *112*, 3495–3502.

(16) Neville, F.; Cahuzac, M.; Kononov, O.; Ishitsuka, Y.; Lee, K. Y. C.; Kuzmenko, I.; Kale, G. M.; Gidalevitz, D. *Biophys. J.* **2006**, *90*, 1275–1287.

(17) Ishitsuka, Y.; Pham, D. S.; Waring, A. J.; Lehrer, R. I.; Lee, K. Y. C. *Biochim. Biophys. Acta* **2006**, *1758*, 1450–1460.

Scheme 1. Structures of Polymer 1 Containing a 2,5-Thienylene Unit in Its Backbone and Phospholipids Used in This Study^a

Compound	Structure	T_m (°C)
Polymer 1		N/A
DLPG (12:0 PG)		-3
DMPG (14:0 PG)		23
DPPG (16:0 PG)		41
DPPC (16:0 PC)		41
DPPE (16:0 PE)		63
DOPG (18:1 PG)		-18

^a Phase transition temperatures, T_m , of the phospholipids are also included. Structures and T_m values were obtained from avantilipids.com.

lipids of varying headgroup or acyl chain length (Scheme 1) to elucidate the effects of lipid headgroup charge and membrane fluidity on polymer-1–membrane interactions. Two model membrane systems are used in this study, small unilamellar vesicles (liposomes) in buffer and lipid monolayers at the air–water interface. A number of techniques were used to study polymer-1–membrane interactions, including fluorescence emission, fluorescence quenching, monolayer insertion assays, and dynamic light scattering. Two series of phospholipids were used. One series is composed of saturated 16-carbon acyl chain lipids with different headgroups, including anionic phosphatidylglycerol (DPPG) lipids, zwitterionic phosphatidylcholine (DPPC) lipids, and zwitterionic phosphatidylethanolamine (DPPE) lipids. The second series contains anionic PG lipids with different acyl chain lengths, including DLPG (12-carbon), DMPG (14-carbon), DPPG (16-carbon), and DOPG (18-carbon). The first series of phospholipids is used to evaluate the effect of lipid headgroup charge, and the second is used to assess the role of lipid fluidity. In order to develop potential antimicrobial or antitumor drugs with minimal toxicity, it is important to understand the underlying principles of the “membrane selectivity” of PPE CPEs.¹⁸

One distinguishing difference between bacterial and human cells is the composition of their cell membranes. The outer leaflet of bacterial membranes contains abundant negatively charged lipids, whereas the outer leaflet of human eukaryotic cell membranes is predominantly zwitterionic.¹⁸ Thus, evaluating the interactions

between the PPE CPEs with model membranes of different headgroup charge will provide some insight into the membrane selectivity of these antimicrobials. The second series of lipids have different phase transition temperatures and thereby display different membrane fluidity at room temperature. The effect of lipid fluidity on the insertion of polymer 1 into lipid membranes has also been evaluated by adjusting the surface pressure of the DPPG monolayer.

Materials and Methods

Lipids and Chemicals. Polymer 1 was prepared according to a previously published procedure.¹⁹ A stock aqueous solution of polymer 1 was prepared by dissolving the polymer powder in water to a concentration of 1.9 mM, expressed as polymer repeat unit concentration (PRU). All lipids were purchased from Avanti Polar Lipids (Alabaster, AL) and used without further purification, including 1,2-dipalmitoyl-*sn*-glycero-3-phosphatidylcholine (DPPC), 1,2-dipalmitoyl-*sn*-glycero-3-phosphatidylethanolamine (DPPE), 1,2-dipalmitoyl-*sn*-glycero-3-[phospho-*rac*-(1-glycerol)] (sodium salt) (DPPG), 1,2-dimyristoyl-*sn*-glycero-3-[phospho-*rac*-(1-glycerol)] (sodium salt) (DMPG), 1,2-dilauroyl-*sn*-glycero-3-[phospho-*rac*-(1-glycerol)] (sodium salt) (DLPG), and 1,2-dioleoyl-*sn*-glycero-3-[phospho-*rac*-(1-glycerol)] (sodium salt) (DOPG). The structures of all the phospholipids as well as their phase transition temperatures, T_m , are shown in Scheme 1. DPPC and DOPG were dissolved in chloroform, and all other phospholipids were dissolved in chloroform containing 10 vol %

(18) Matsuzaki, K.; Sugishita, K.-i.; Fujii, N.; Miyajima, K. *Biochemistry* **1995**, *34*, 3423–3429.

(19) Chemburu, S.; Ji, E.; Casana, Y.; Wu, Y.; Buranda, T.; Schanze, K. S.; Lopez, G. P.; Whitten, D. G. *J. Phys. Chem. B* **2008**, *112*, 14492–14499.

methanol. The concentration of phospholipid solutions was 2 mM for those used to prepare liposomes and between 0.3 and 0.4 mg/mL for those used to spread at the air–water interface to prepare lipid monolayers. All lipid solutions were stored at $-20\text{ }^{\circ}\text{C}$ in glass vials. A $10\times$ stock phosphate buffered saline (PBS) solution was prepared and subsequently diluted 10-fold to use for all fluorescence experiments. Langmuir trough experiments were carried out on the water subphase. The $1\times$ PBS solution contained 0.137 M NaCl, 2.68 mM KCl, 10.1 mM Na_2HPO_4 , and 1.76 mM KH_2PO_4 . The pH of the PBS was adjusted to 7.4 using 1 M HCl. The quencher, 9,10-anthraquinone-2,6-disulfonic acid (AQS), was purchased from Sigma-Aldrich and was dissolved in water to a concentration of 5 mM. The water used throughout the study is ultrapure Milli-Q water with a resistivity of $18.2\text{ M}\Omega\text{ cm}^{-1}$.

Preparation of Liposomes. Small unilamellar vesicles (liposomes) were prepared by an extrusion method using 2 mM lipid solutions. Liposome preparation includes the following steps: generating lipid thin films on vial walls by evaporating the organic solvents, hydrating lipid films with PBS to 2 mM under strong shaking for 1 h, freeze–thawing the lipid–buffer suspension using a dry ice bath and warm water for five cycles, and finally homogenizing the liposomes by extruding the suspensions through 100 nm polycarbonate filters using a mini-extruder (Avanti Polar Lipids, Alabaster, AL) for 11 passes. For DPPC and DOPG lipids dissolved in chloroform, the organic solvent was evaporated under vacuum. For all other lipids dissolved in the chloroform–methanol mixture, samples were first dried using a rotary evaporator and then further dried under vacuum. For both the hydration and extrusion processes, lipid solutions were kept at temperatures above each lipid's T_m (Scheme 1).

Preparation of Polymer–Liposome Mixtures. Polymer–liposome mixtures were prepared by first mixing liposomes with 1 vol % stock polymer **1** solution to a final concentration of 1.9 mM, followed by 30 min of vigorous shaking at a temperature higher than the T_m of the lipid. DLPG, DMPG, and DOPG liposome mixtures with polymer **1** were prepared at room temperature, DPPG and DPPC mixtures with polymer **1** were prepared at $52\text{ }^{\circ}\text{C}$, and DPPE mixture with polymer **1** was prepared at $70\text{ }^{\circ}\text{C}$.

Fluorescence Assays. Fluorescence measurements of polymer–liposome mixtures and polymer alone were acquired using a SpectroMax M-5 microplate reader (Molecular Devices, Sunnyvale, CA). A 96-well plate (BD Falcon, white/clear bottom) was used, and 100 μL of each sample was analyzed. The excitation wavelength for either polymer or polymer–liposome samples was 420 nm, and the emission was collected from 460 to 700 nm.

Dynamic Light Scattering Measurements. The hydrodynamic radius (R_h) of liposomes and polymer–liposome mixtures was measured using a WyattQELS light scattering instrument (DAWN HELEOS II, Wyatt Technology Corporation, Santa Barbara, CA). A linearly polarized gallium arsenide laser was used as the light source (658 nm at 130 mW). Liposome samples and the polymer–liposome mixtures were diluted 50-fold for dynamic light scattering measurements. The R_h was extrapolated using a cumulant analysis, which assumes that the scattering species are spherical and monodisperse.

Monolayer Insertion Assays. Monolayer insertion assays were performed on a Langmuir trough equipped with a Wilhelmy plate and two identical mobile Delrin barriers (KSV Instruments, Monroe, CT). The water subphase volume was 50 mL, and the maximum working surface area was 100 cm^2 . Polymer insertion experiments were carried out either at a constant surface pressure or a constant surface area. Lipids were first spread at the air–water interface using a glass microsyringe (Hamilton, Reno, NV) and left undisturbed for 15 min to completely evaporate the organic solvent. Then the lipid monolayer was compressed to a target pressure, and either the surface area or surface pressure was held constant. Polymer **1** (50 μL of stock solution) was then injected underneath the monolayer using a microsyringe to a final

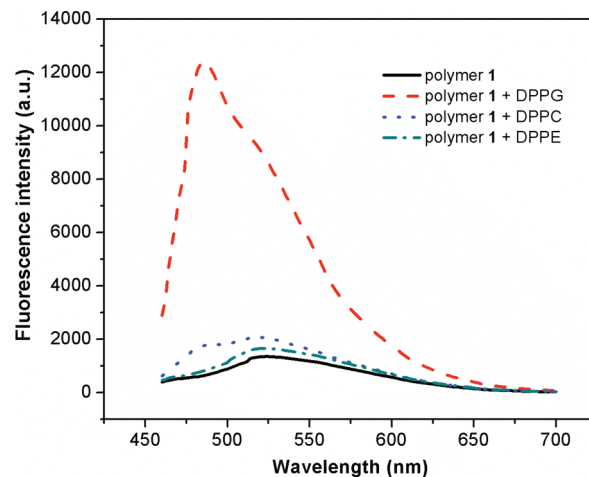


Figure 1. Fluorescence spectra of polymer **1** (solid black line) and its mixtures with DPPG (red dashed line), DPPC (blue dotted line), and DPPE (green dash-dotted line) liposomes ($\lambda_{\text{ex}} = 420\text{ nm}$).

subphase concentration of $1.9\text{ }\mu\text{M}$. The system was left undisturbed for the polymer to equilibrate with the lipid monolayer. The insertion of polymer **1** into the lipid monolayer resulted in either an increase in film area for constant-pressure insertion experiments or an increase in surface pressure for constant-area insertions experiments. Film area and surface pressure were recorded as a function of time. For constant-pressure insertion experiments, three surface pressures were used, 20, 25, and 30 mN/m. Surface pressures were kept constant by adjusting the position of the barriers via a feedback loop. For constant-surface-area insertion experiments, the lipid films were first compressed to a target surface pressure of 25 mN/m and then the barriers were stopped to maintain a constant surface area.

Results and Discussion

Lipid Headgroup Charge Effect: Fluorescence Studies. As found in our previous study, the cationic PPE polymer **1** exhibits strong affinity toward PG membranes, possibly due to favorable electrostatic interaction between cationic polymer **1** and the anionic PG membrane.¹⁴ Therefore, it is important to determine the effect of lipid headgroup charges on the polymer–membrane interactions. The results will help to provide an understanding of the membrane selectivity of polymer **1** and evaluate its potential as a biocide.¹⁷ To this end, the interactions between polymer **1** and three phospholipids with different headgroups, but identical acyl chains, were evaluated. The lipids used are the anionic DPPG lipid and the zwitterionic DPPC and DPPE lipids. Liposomes were prepared and used as a model bilayer membrane system.²⁰ Each liposome was then mixed and incubated with polymer **1**. Fluorescence measurements of these liposome–polymer samples were made to monitor any fluorescence changes of polymer **1** due to its interactions with the liposomes (Figure 1).

As shown in Figure 1, mixing polymer **1** with DPPG liposomes leads to a large fluorescence increase (ca. 10 times) and a significant blue shift of the polymer emission peak maximum from 520 to 484 nm. This result is consistent with our previous finding that mixing polymer **1** with anionic DOPG liposomes induced fluorescence enhancement and spectral shift that are attributable to the conformational change of polymer **1** from an aggregated state to a more extended state upon associating with DOPG membrane and then inserting into the hydrophobic acyl

(20) Pérez-López, S.; Vila-Romeu, N.; Esteller, M. A. A.; Espina, M.; Haro, I.; Mestres, C. *J. Phys. Chem. B* **2009**, *113*, 319–327.

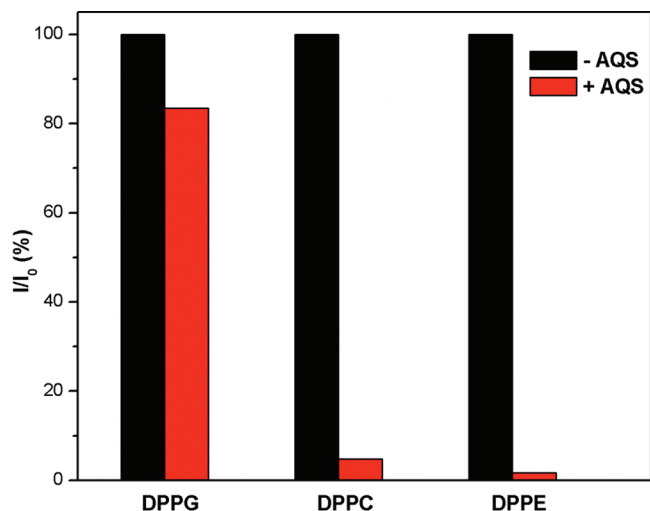


Figure 2. Fluorescence quenching of polymer **1** by AQS in the presence of DPPG, DPPC, and DPPE liposomes. I and I_0 are the polymer fluorescence with and without AQS, respectively.

chain region of the lipid bilayer.¹⁴ In contrast, mixing polymer **1** with the neutrally charged DPPC or DPPE liposomes does not lead to significant changes in the polymer's fluorescence (Figure 1). For DPPE, there is little variation in either the fluorescence intensity or the fluorescence spectrum profile. Mixing polymer **1** with DPPC, however, induces only a small increase in fluorescence intensity and added a new peak to the emission spectrum at ca. 484 nm. This blue shift of the polymer emission peak indicates that polymer **1** has inserted into the hydrophobic interiors of the DPPC liposomes. However, the weak emission intensity of the new peak suggests that the amount is quite small. Therefore, changes in polymer **1** fluorescence when mixed with the zwitterionic DPPC liposomes do not induce significant conformational changes of polymer **1**. The lack of polymer **1** conformational changes indicates that there are little interactions between polymer **1** and the zwitterionic lipid membranes. The small difference between polymer **1**'s fluorescence when mixed with DPPC and DPPE may arise from the difference in hydrophobicity between choline and ethanolamine in the lipid headgroups, where the former is slightly more hydrophobic and better able to induce polymer **1**'s conformation to change.

To better understand the interactions between polymer **1** and lipids with different headgroup charges, fluorescence quenching by AQS was also measured. AQS is an anionic superquencher to the fluorescence emission of PPE CPEs, where Stern–Volmer constants in excess of 10^5 M^{-1} have been routinely observed.^{21,22} The fluorescence intensity of polymer **1** mixed with the three liposomes was recorded at 484 nm before and after the addition of AQS. The final concentration of AQS was 0.1 mM, and this concentration was sufficient to quench 19 μM polymer **1** in PBS. The fluorescence emission at 484 nm of polymer–liposome mixtures was measured before (I_0) and after the addition of AQS (I). I/I_0 , which reflects the percentage of unquenched polymer, of each polymer–liposome mixture is presented in Figure 2.

As shown in Figure 2, the addition of AQS results in more than 90% decrease of the polymer emission when mixed with DPPC and DPPE liposomes, that is, 10% of the polymer's fluorescence

was unquenched. In contrast, AQS does not significantly quench the polymer emission when mixed with DPPG liposomes, where 85% of the polymer fluorescence remained unquenched. These results imply that polymer **1** is easily accessible to the AQS molecules when mixed with DPPC and DPPE liposomes but the polymer becomes largely shielded from the quencher when it is mixed with DPPG liposomes. As suggested in our previous study,¹⁴ the shielding effect of the DPPG liposomes could be due to the insertion of polymer **1** into the lipid bilayers of liposomes and the subsequent translocation into the interior of the liposomes. On the other hand, the near complete quenching of polymer **1** by AQS reflects that there is little polymer incorporation into DPPC and DPPE liposomes.¹³ The slightly higher shielding effect of DPPC compared to DPPE is consistent with the difference in fluorescence spectra in Figure 1, indicating that only a small amount of polymer **1** is incorporated into the DPPC liposomes.

The combined results from polymer **1** fluorescence spectra and fluorescence quenching show that the cationic PPE polymer **1** preferentially interacts with the anionic PG membrane over the zwitterionic DPPC and DPPE membranes. Our results demonstrate that electrostatic interactions play a key role mediating cationic PPEs–membrane interactions. Compared with zwitterionic lipids, anionic lipids have been shown to enhance an antimicrobial peptide's association with and insertion into lipid membranes.²³ Apparently, we are observing a similar phenomenon for polymer **1**. It is also well-known that bilayers of zwitterionic lipids resist the adsorption of macromolecules such as proteins.²⁴ Thus, the combination of favorable electrostatic interactions between polymer **1** and anionic PG membranes and the resistance of zwitterionic membranes toward macromolecular adsorption²⁴ may give rise to polymer **1**'s selective affinity toward the different liposomes studied. The significant association and insertion of polymer **1** into PG lipid membranes can disrupt membrane lipid packing and organization, which may account for its dark biocidal activity. Moreover, polymer **1**'s selectivity makes it an attractive antimicrobial candidate, as it may have the ability to selectively and effectively kill bacterial cells but exhibit low toxicity toward eukaryotic cells, including mammalian cells. As described previously, the outer leaflets of eukaryotic membranes are exclusively composed of zwitterionic phospholipids whereas the bacterial membranes are abundant in anionic phospholipids, such as PG lipids.¹⁸

Lipid Headgroup Charge Effect: Constant-Area Insertion Assays. The ability of polymer **1** to incorporate into lipid membranes can be quantitatively determined by measuring its insertion into lipid monolayers at the air–water interface held at a constant surface pressure or constant surface area. For a constant-area measurement, the lipid monolayer is first compressed to a target surface pressure of 25 mN/m and then the barriers are stopped to maintain a constant surface area. The polymer is then injected in the subphase underneath the monolayer, and the subsequent insertion of the polymer into the monolayer film results in increases in monolayer surface pressure. This is a straightforward method to monitor membrane insertion and has been employed to study antimicrobial polymers or peptides.^{13,25} In this study, the insertion of polymer **1** into DPPG, DPPC, and DPPE monolayers was evaluated by the constant area insertion assays in order to further understand the membrane selectivity of polymer **1**.¹⁷ The

(21) Zeineldin, R.; Piyasena, M. E.; Sklar, L. A.; Whitten, D.; Lopez, G. P. *Langmuir* **2008**, *24*, 4125–4131.

(22) Zeineldin, R.; Piyasena, M. E.; Bergstedt, T. S.; Sklar, L. A.; Whitten, D.; Lopez, G. P. *Cytometry, Part A* **2006**, *69*, 335–341.

(23) Chi, E. Y.; Ege, C.; Winans, A.; Majewski, J.; Wu, G.; Kjaer, K.; Lee, K. Y. *C. Protein* **2008**, *72*, 1–24.

(24) Glasmästar, K.; Larsson, C.; Höök, F.; Kasemo, B. *J. Colloid Interface Sci.* **2002**, *246*, 40–47.

(25) Maskarinec, S. A.; Lee, K. Y. *C. Langmuir* **2003**, *19*, 1809–1815.

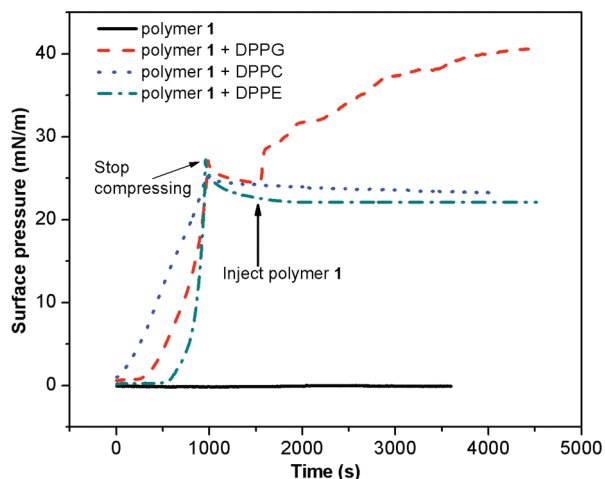


Figure 3. Constant-area measurements of DPPG, DPPC, and DPPE monolayers after injecting polymer **1** into the water subphase.

results are shown in Figure 3. All three lipid monolayers, DPPG, DPPE, and DPPC, are in the liquid condensed phase at 25 mN/m at room temperature (Figure S-1 in the Supporting Information). As a control, the surface pressure reached by the adsorption of polymer **1** to the air–water interface, without a lipid monolayer, was also determined to assess the inherent surface activity of the polymer.

As shown in Figure 3 (black line), polymer **1** alone did not give rise to any surface pressure at the air–water interface after it is injected into the subphase for over 1 h. This result implies that polymer **1** does not exhibit any surface activity at the concentration used in our experiments. In contrast, injecting polymer **1** in the subphase beneath a DPPG monolayer immediately induced increases in the lipid monolayer's surface pressure and resulted in a 15 mN/m increase over a period of 1 h (red dashed line in Figure 3). However, when polymer **1** was injected in the subphase beneath either the DPPE or DPPC monolayer, no changes in surface pressure were observed. Although the amount of polymer **1** that had inserted into the DPPG membrane cannot be estimated by the current method, it is reasonable to expect that the polymer's insertion can cause alterations in the packing and organization of the DPPG lipids, possibly leading to membrane damage. On the contrary, the lack of any surface pressure increase when the polymer was injected underneath DPPC and DPPE monolayers implies that polymer **1** did not insert into these two membranes. This is consistent with the results obtained from fluorescence measurements. The observed difference in the insertion of polymer **1** into the differently charged lipids with identical tail groups is analogous to the results obtained through fluorescence measurements of the association of polymer **1** with liposomes as discussed above. Polymer **1** interacts strongly with anionic lipids and exhibits no interactions toward zwitterionic lipids. This charge selectivity may be the dominant factor attributing to the biocidal action of polymer **1**.

Lipid Packing (Fluidity) Effect: Constant-Pressure Insertion Assays. The ability of polymer **1** to insert into DPPG monolayers held at different surface pressures was also investigated. Three different surface pressures, 20, 25, and 30 mN/m, were used to provide different lipid packing in the monolayers. The monolayer was first compressed to a target pressure and then kept constant via a feedback loop. After a 10 min equilibration time, polymer **1** was injected in the water subphase underneath the lipid monolayer. Since the monolayer is maintained at constant

Table 1. Percent Area Expansion of the DPPG Monolayer Held at Different Surface Pressures Induced by the Insertion of Polymer **1**^a

surface pressure (mN/m)	$\Delta A/A_0$ (%)
20	65.5
25	45.1
30	33.3

^a[Polymer **1**] = 1.9 μ M; T = 25 $^{\circ}$ C; subphase = water.

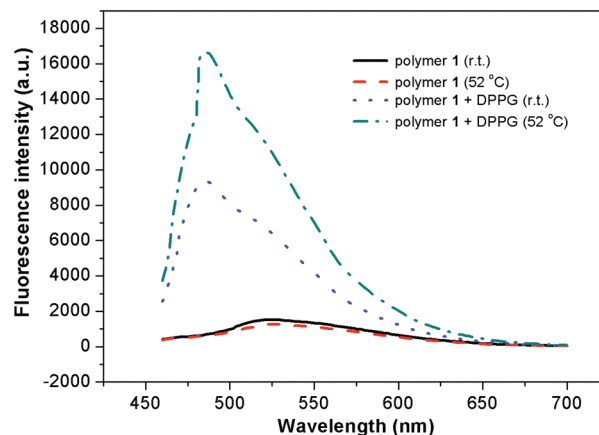


Figure 4. Fluorescence spectra of polymer-**1**–DPPG liposomes mixture prepared at temperatures below (room temperature) and above (52 $^{\circ}$ C) the lipid's phase transition temperature at 42 $^{\circ}$ C.

pressure, the barriers expand as a result of polymer insertion. The monolayer surface area was recorded as a function of time and the percent area expansion ($\Delta A/A_0$, where $\Delta A = A_f - A_0$. A_0 is the monolayer surface area before polymer insertion, and A_f is the monolayer surface area after 1 h of polymer insertion) was calculated.

Polymer **1** spontaneously and efficiently inserted into a DPPG monolayer held at constant pressures (Figure S-2 in the Supporting Information). $\Delta A/A_0$ results are summarized in Table 1. Each data point represents the area expansion over a period of 1 h. It can be seen that polymer **1** inserted into the DPPG monolayer held at all three surface pressures and that $\Delta A/A_0$ decreased with increasing surface pressure. It is known that higher surface pressures result in tighter acyl chain packing.¹⁷ As shown here, increasing lipid packing density, or decreasing membrane fluidity, reduces the insertion of polymer **1** into the lipid membrane. This result suggests that, in addition to lipid headgroup charge, lipid packing density also plays a role in determining the extent of polymer insertion into the membrane.

In addition to varying the surface pressure to adjust lipid packing, altering the temperature can also change the fluidity of liposome membranes. The fluidity of a bilayer significantly increases when the temperature is raised above its phase transition temperature (T_m). The T_m value for DPPG is 41 $^{\circ}$ C. Therefore, the DPPG bilayer is in the gel phase with low acyl chain mobility at temperatures below 41 $^{\circ}$ C and in the liquid phase with higher acyl chain mobility at temperatures above 41 $^{\circ}$ C. To determine the effect of membrane fluidity on polymer–membrane interactions, polymer–DPPG liposome mixtures were prepared at room temperature, below the T_m , and at 52 $^{\circ}$ C, above the T_m . The fluorescence emission spectra of the polymer–liposome mixture at the two temperatures as well as those of the polymer alone are shown in Figure 4. As shown, the fluorescence intensity of polymer **1** remains largely unchanged when the temperature is increased from room temperature to 52 $^{\circ}$ C. Interestingly, the same increase in temperature roughly doubled the fluorescence

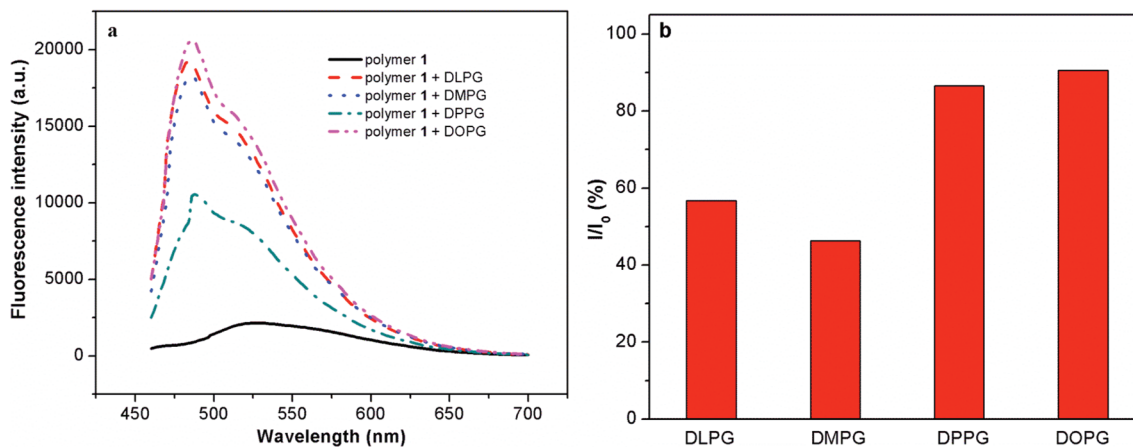


Figure 5. (a) Fluorescence emission spectra of and (b) fraction of the fluorescence of **1** remaining after AQS addition to mixtures of polymer **1** with PG liposomes.

intensity of polymer **1** when it is mixed with DPPG liposomes (Figure 4). As discussed earlier, the fluorescence enhancement of polymer **1** is due to the conformational changes polymer **1** undergoes when it becomes incorporated (insertion and translocation) into anionic liposomes. Since increasing the amount of polymer inserted into the liposomes and increasing the extent of polymer conformational changes influence the degree of fluorescence enhancement, both can contribute to the polymer's increased fluorescence emission at 52 °C (Figure 4). Fluorescence quenching experiments showed that AQS exhibits similar quenching efficiency toward the emission of polymer **1** when it is mixed with DPPG liposomes either at room temperature or at 52 °C, where roughly 20% of polymer emission was quenched (data not shown), suggesting that similar amounts of polymer **1** become incorporated into the liposomes at both temperatures. Thus, the enhanced polymer fluorescence emission at the higher temperature is mainly due to the ability of the membrane, once the polymer becomes associated to the membrane surface, to induce the polymer to adopt a more extended conformation, or become more “dissolved” in the membrane. Since increasing the temperature of the liposomes to above its T_m significantly increases acyl chains mobility and thus membrane fluidity, our results show that membrane fluidity plays an important role in modulating polymer–membrane interactions.

Lipid Bilayer Thickness Effect. A series of PG liposomes (DLPG, DMPG, and DPPG) were prepared to examine the effect of lipid bilayer thickness on their interactions with polymer **1**. The lipid hydrophobic thickness is a well-known parameter that modulates protein–membrane interactions (hydrophobic matching).²⁶ The acyl chain lengths of the PG lipids ranged from 12 to 16 carbons; the acyl chain thicknesses are 6.29 Å for the 12-carbon DLPG, 7.43 Å for the 14-carbon DMPG, and 8.57 Å for the 16-carbon DPPG.²⁶ In addition to the saturated PG lipids, a lipid with unsaturated tails, DOPG, was also used (Scheme 1). Note that the different lipids also have different T_m values (Scheme 1). Thus, in addition to membrane thickness, polymer **1** also experiences different lipid fluidity when mixed with these PG liposomes. All polymer–liposome mixtures were prepared at room temperature.

Figure 5a presents the fluorescence emission spectra of polymer **1** mixed with different PG liposomes. It can be seen that all the PG liposomes induced fluorescence enhancement as well as a blue shift of the emission maximum of polymer **1**. This indicates again

that the electrostatic attraction between the cationic PPE polymer and anionic PG lipids induces the polymer to undergo conformational changes from an aggregated state in an aqueous environment to a more extended state.^{14,27} The identical emission peak maximum wavelength for all polymer–liposome samples implies that, when mixed with the liposomes, polymer **1** exists in a similar chemical environment, which is more hydrophobic compared to the aqueous buffer. This could be attributed to the insertion of polymer **1** into the hydrophobic tail region of the liposome bilayer. The fluorescence intensity shows the following order: DOPG > DLPG > DMPG \gg DPPG. The fluorescence of polymer **1** with DPPG (at room temperature) is much weaker compared to those from the other three lipids, consistent with earlier results. The trend in fluorescence intensity is the same as the trend in liposome membrane fluidity or T_m values (Scheme 1). This result implies again that increasing membrane fluidity favors the conformational changes of polymer **1** from an aggregated state to a more extended state after being incorporated in the PG bilayers.

Figure 5b shows the fluorescence quenching results of AQS to the above-mentioned polymer–liposome mixtures. The ratio I/I_0 reflects the percentage of unquenched polymer. From Figure 5b, it is clear that lipids containing longer tail groups more effectively shield polymer **1** from quenching by AQS. DPPG and DOPG liposomes protect around 85% of polymer **1** from being quenched by AQS. However, the shielding effects of DLPG and DMPG liposomes are lower, as less than 60% and 50% of polymer fluorescence were retained. These results indicate that the thicker DPPG and DOPG bilayers are more efficient at shielding the incorporated polymer from AQS than the thinner DLPG and DMPG membranes. The 16-carbon acyl chains of DPPG are 15% and 36% thicker than those of DMPG and DLPG, respectively.²⁶ Our results suggest that liposome bilayer thickness plays a critical role in the incorporation of polymer **1** into the lipid membrane. The general trend emerging is that thicker bilayers are able to take up more polymers. The slightly higher protection efficiency of DLPG liposomes than DMPG liposomes may arise from the more fluid nature of the DLPG liposomes. The different trends in polymer **1** fluorescence enhancement and fluorescence quenching screening by PG liposomes suggest that the conformational changes of polymer **1** are highly mediated by the fluidity of the lipid bilayer, whereas the amount of polymer incorporated into the bilayers is mediated by bilayer thickness.

(26) Sperotto, M. M.; Mouritsen, O. G. *Eur. Biophys. J.* **1988**, *16*, 1–10.

(27) Liu, Y.; Ogawa, K.; Schanze, K. S. *Anal. Chem.* **2008**, *80*, 150–158.

Table 2. Hydrodynamic Radii of Liposomes before and after the Addition of Polymer 1

liposomes	R_h (nm)	liposome–polymer-1 mixtures	R_h (nm)	ΔR_h (nm)
DLPG	47.7 ± 1.1	DLPG/polymer 1	57.3 ± 2.5^a	9.6 ± 2.7
DMPG	50.8 ± 1.6	DMPG/polymer 1	57.4 ± 4.4^a 54.2 ± 2.6^b	6.6 ± 4.7 3.4 ± 3.0
DPPG	48.7 ± 1.6	DPPG/polymer 1	54.5 ± 1.9^a 52.1 ± 2.0^b	5.8 ± 2.5 3.4 ± 2.6
DOPG	53.4 ± 1.5	DOPG /polymer 1	56.0 ± 2.3^a	2.6 ± 2.7

^a Samples prepared at room temperature. ^b Samples prepared at a temperature above the T_m of each lipid (33 °C for DMPG and 52 °C for DPPG).

Dynamic Light Scattering Investigation of Liposome Size Variation. The association and further incorporation of polymer 1 into PG liposomes may induce measurable changes in liposome size distribution. To evaluate changes in liposome size with the addition of polymer 1, the hydrodynamic radii (R_h) of polymer–liposome samples were measured by dynamic light scattering. As controls, R_h values of the liposomes alone were also determined. The light scattering data are summarized in Table 2. All of the control samples exhibit a size of approximately 100 nm in diameter with a fairly narrow size distribution. This is reasonable, since 100 nm pore size polycarbonate filters were used to extrude the liposomes. The addition of polymer 1 to the different liposomes causes increases in the size of all PG liposomes, suggesting the association of polymer 1 to the liposome surface. Interestingly, the order of vesicle size increase is as follows: DLPG (9.6 nm) > DMPG (6.6 nm) > DPPG (5.8 nm) > DOPG (2.6 nm) when PG liposomes were mixed with polymer 1 at room temperature. When the mixing temperature is well above T_m , polymer–liposome mixtures of DMPG and DPPG show a smaller size increase (3.4 nm) compared to samples prepared at room temperature, below T_m (6.6 and 5.8 nm). The larger increases in the sizes of DLPG and DMPG liposomes with

polymer addition may be due to their thinner membranes, where more of the polymers remain on the exterior of the bilayer membrane. This interpretation is also consistent with the results from fluorescence quenching measurements. The smaller increases in the liposome sizes when liposome–polymer mixtures are prepared at a temperature above T_m indicate again that the more fluid membranes can efficiently take up polymer 1 into the membrane bilayer. This also explains why the DOPG–polymer-1 mixture has the smallest size increase since DOPG liposome is the most fluid membrane.

Conclusions

The results obtained from the investigation of an antimicrobial cationic conjugated polyelectrolyte (polymer 1) with two model lipid membranes, liposomes and lipid monolayers, demonstrate that polymer 1 exhibits selective affinity toward anionic PG lipid membranes over zwitterionic PE and PC membranes, which makes polymer 1 an attractive antimicrobial material in potential applications since the selective targeting of PG lipids over zwitterionic lipids of polymer 1 may correlate with an ability to selectively target bacteria cells over human cells. Our study shows that the fluidity of the lipid membranes and lipid packing play important roles in mediating polymer–membrane interactions. The conformational change of polymer 1 upon interacting with lipid membrane and the extent of polymer insertion into membranes are favored by increasing membrane fluidity.

Acknowledgment. This research is financially supported by the Defense Threat Reduction Agency (Contract No. W911NF07-1-0079). L.D. would like to thank the National Natural Science Foundation of China (No. 20803046) for support.

Supporting Information Available: Surface-pressure–area isotherms of DPPG, DPPE, DPPC, and that of DPPG in the presence of polymer 1. These materials are available free of charge via the Internet at <http://pubs.acs.org>.